

stable for at least 8 months as shown by the invariance of  $k_1$  measured using the same sample but 8 months apart.) In some of the earlier studies,  $\text{CH}_3\text{CCl}_3$  may have decomposed upon heating or on metal cell walls. We also have observed that the formation of  $\text{CH}_2\text{CCl}_2$  is enhanced in the presence of water adsorbed on surfaces. Nelson *et al.* (16) used approximately 12 torr of  $\text{H}_2\text{O}$  to produce OH, and they could have inadvertently generated  $\text{CH}_2\text{CCl}_2$ .

Our results indicate that the previously accepted values of  $k_1$  are too high above 240 K. The lower values of  $k_1$  at tropospheric temperatures increase the OH concentrations estimated from the  $\text{CH}_3\text{CCl}_3$  budget analysis. This increase, in turn, decreases the calculated tropospheric lifetimes of molecules whose primary loss is via reaction with OH. The magnitude of the change can be roughly gauged from the values of  $k_1$  at 277 K, which is an approximate average of the temperature at which the OH-initiated degradation of a well-mixed tropospheric gas takes place. Our value of  $k_1$  at 277 K is ~15% lower than the earlier recommendations. Examples of the implications of the new value of  $k_1$  include (i) a decrease in the calculated atmospheric lifetime of  $\text{CH}_4$  by 15% and a 15% increase in its flux to balance the larger atmospheric loss rate, and (ii) decreases in the calculated lifetimes of hydrofluorocarbons and hydrofluorochlorocarbons (HCFCs) and ozone depletion potentials of HCFCs, the proposed CFC substitutes, by 15%. In the case of  $\text{CH}_4$ , the new value of  $k_1$  will partially offset the balance in its budget that was calculated after our report on the OH +  $\text{CH}_4$  reaction (8).

*Note added in proof:* DeMore (17) and Finlayson-Pitts *et al.* (18) have also recently measured  $k$ , to be substantially the same as that reported here

## REFERENCES AND NOTES

1. P. Midgley, *Atmos. Environ.* **23**, 2663 (1989).
2. J. H. Butler *et al.*, *J. Geophys. Res.* **96**, 22347 (1991).
3. R. Prinn *et al.*, *ibid.* **97**, 2445 (1992).
4. W. B. DeMore *et al.*, *Chemical Kinetics and Photochemical Data for Use in Stratospheric Modeling* (Evaluation No. 9, JPL Publ. 90-1, Jet Propulsion Laboratory, Pasadena, CA, 1 January 1990).
5. R. Atkinson *et al.*, *J. Chem. Phys. Ref. Data* **18**, 881 (1989).
6. M. J. Kurylo, P. C. Anderson, O. Klais, *Geophys. Res. Lett.* **6**, 760 (1979).
7. K.-M. Jeong and F. Kaufman, *ibid.*, p. 757.
8. G. L. Vaghjiani and A. R. Ravishankara, *Nature* **350**, 1 (1991).
9. ———, *J. Phys. Chem.* **93**, 1948 (1989).
10. T. Gierczak, R. Talukdar, G. L. Vaghjiani, E. R. Lovejoy, A. R. Ravishankara, *J. Geophys. Res.* **96**, 5001 (1991).
11. A. Wahner and A. R. Ravishankara, *ibid.* **92**, 2189 (1987).
12. N. Vanlaethem-Meurée, J. Wisenberg, P. C. Simon, *Geophys. Res. Lett.* **6**, 451 (1979).
13. R. K. Talukdar, A. Mellouki, A. R. Ravishankara, in preparation.
14. The rate coefficient for the reaction of OH with 1,1-dichloroethane cannot be larger than that for the reaction of OH with  $\text{C}_2\text{H}_6$ . We have used the rate coefficient for the OH +  $\text{C}_2\text{H}_6$  reaction (4) in placing the limit for the contribution of the OH + 1,1-dichloroethane reaction to the measured value of  $k_1$ . The rate coefficient for the reaction of OH with  $\text{CHCl}_2\text{CCl}_2$  is from (4).
15. A. A. Turnipseed, G. L. Vaghjiani, J. E. Thompson, A. R. Ravishankara, *J. Chem. Phys.* **96**, 5887 (1992).
16. L. Nelson, I. Shanahan, H. W. Sidebottom, J. Treacy, O. J. Nielsen, *Int. J. Chem. Kinet.* **22**, 577 (1990).
17. W. DeMore *Geophys. Res. Lett.*, in press.
18. B. J. Finlayson-Pitts *et al.*, *ibid.*, in press.
19. This research was funded in part by the National Oceanic and Atmospheric Administration's climate and global change program. We are grateful to Dow Chemicals and C. Nieme for the analyzed samples of  $\text{CH}_3\text{CCl}_3$ .

30 March 1992; accepted 18 May 1992

## Microaggregations of Oceanic Plankton Observed by Towed Video Microscopy

Cabell S. Davis, Scott M. Gallager, Andrew R. Solow

Oceanic plankton have been hypothesized to occur in micropatches (<10 meters) that can have a large impact on marine ecosystem dynamics. Towed video microscopy was used to unobtrusively determine distributions of oceanic plankton over a continuum of scales from microns to hundreds of meters. Distinct, taxa-specific aggregations measuring less than 20 centimeters were found for copepods but not for nonmotile (cyanobacterial colonies) or asexual (doliolid phorozooids) forms, which suggests that these small patches are related to mating. Significant patchiness was also found on larger scales and was correlated among taxa, indicating physical control. These video observations provide new insights into basic plankton ecology by allowing quantitative assessment of individual plankton in their natural, undisturbed state.

The microscale (<10 m) environment of oceanic plankton is thought to be important in determining population and ecosystem dynamics (1, 2). Foraging models have shown that microscale patchiness in prey density can greatly enhance predator population growth (3, 4). In laboratory experiments, the abundance of prey required for maximal growth of predators is often well above that found in the field; the body size and the growth rate of field predators, however, are similar to those of laboratory animals grown in saturating food (1, 5). This discrepancy is hypothesized to be a result of field predators feeding in micropatches of prey that are too small to resolve with existing instrumentation (1, 4-6).

Spatial distributions in oceanic plankton on scales from microns to hundreds of meters were determined with the use of the newly developed video plankton recorder (VPR) (7). The VPR was equipped with conductivity, temperature, pressure, and flow sensors and was towed at 0.75 to 2.25 m/s near the surface (1 to 8 m) and outboard (7 m) of the side of the ship. Video recordings were scanned visually at 5 to 30 fields per second to detect the presence of organisms, and when they were found, taxa and time code were noted. Tow speed data from the flow sensor were used to convert the time code to distance along the tow path.

Tows were made from the R.V. *Oceanus* on 29 and 30 August 1991 in continental shelf (70 m bottom depth; 40°41'N, 70°33'W) and slope (39°32'N, 70°00'W) waters south of Woods Hole, Massachusetts. A tow from each area was analyzed for the presence of micropatchiness. Satellite infrared imagery together with VPR data on sea surface temperature and salinity indicated the slope station was positioned in the western edge of a warm-core Gulf Stream ring. Seas were calm, with the result that the wind-induced turbulent mixing rate was minimal, favoring micropatch formation (4).

The unobtrusive nature of the VPR (8) enabled observation and quantification of delicate forms that have typically been difficult or impossible to sample with traditional gear such as nets, pumps, and Niskin bottles. These forms included cyanobacterial colonies (Fig. 1A), marine snow, copepods carrying egg clutches, doliolids with buds (Fig. 1B), medusae, ctenophores, larvaceans (Fig. 1F), sarcodines, salp chains, and large, chain-forming diatoms. Such forms can have a large impact on marine ecosystem dynamics, but little is known of their abundance and distribution. Large amounts of nitrogen-fixing cyanobacterial colonies, *Trichodesmium* sp. (Fig. 1A), were found along the transect in the warm-core ring (Fig. 2), which supports the view that they are potentially a major source of new nitrogen and organic carbon in open ocean areas (9). Likewise, gelatinous forms such as the tunicate *Doliolum nationalis* (Fig. 1B) were found in dense patches along the

C. S. Davis and S. M. Gallager, Department of Biology, Woods Hole Oceanographic Institution, Woods Hole, MA 02543.  
A. R. Solow, Department of Marine Policy, Woods Hole Oceanographic Institution, Woods Hole, MA 02543.

shelf transect (Fig. 2), which indicates that these species may be dominant grazers of phytoplankton (10).

Important observations of individuals include vertical orientation (cyclopoid copepods were always oriented in a head-

down position, perhaps a predator avoidance behavior) (Fig. 1C), body segmentation (Fig. 1, D and E), external parasites (*Centropages* covered with stalked epizoans), and internal lipid sacs and gut masses (Fig. 1, D and E). Such observations can be used in the future to provide in situ indices for life history parameters.

To analyze distributional patterns, we determined from the video the locations of individuals of different taxa along each of the two transects. Because the occurrence of more than one individual in a single video field was rare (and the fields were nonoverlapping), the data for each transect represented a binary (presence or absence) spatial sequence. Distributions of plankton on scales >10 m (Fig. 2) reveal large fluctuations (greater than fivefold) in all groups on scales of 20 m; larger scale trends (>100 m) also were found. Doliolids were the most variable group at the larger scales and were distributed in two large, distinct patches of 100 and 180 m (Fig. 2).

Patchiness as a function of spatial scale was determined for both transects by the use of a point process method (11). Aggregations at scales <20 cm were found for all groups of copepods but not for the nonmotile cyanobacterial colonies *Trichodesmium* sp. or for the asexual (phorozoid) life stage of doliolids (Fig. 2). Although microaggregations <20 cm were found for all groups of copepods, abundances were not correlated ( $P > 0.05$ ) between the groups at these scales. These results indicate that the small micropatches were formed by active swimming and are monogenic. It is likely that these small patches are monospecific and represent social aggregations related to mating. The resolution of the video images, however, was not sufficient to identify organisms at the species level.

Significant patchiness was observed at larger scales as well. Micropatchiness on scales of 1 to 5 m was found for all groups except *Centropages* (Fig. 2). Such aggregations can have profound impacts on predator-prey interactions in the plankton because predators can migrate quickly, moving in a modified random walk, up a concentration gradient of prey and feed at increased rates (4). Microscale turbulence can dissipate such patches, however, and the small-scale patchiness we observed under calm conditions may not occur in situations of high wind or tidal mixing. Turbulence may adversely affect reproductive potential in plankton populations by preventing the formation of mating aggregations. Future comparative studies are planned in both turbulent and quiescent environments. Large-scale trends in abundance (10 to 200 m) also were observed for all groups (Fig. 2). Significant correlations ( $P < 0.05$ ) were found between *Oithona* and *Centropages*

**Fig. 1.** Video images of plankton taken with the VPR while towing at 1 m/s. (A) Cyanobacterial colony, *Trichodesmium* sp. (from ring transect). (B) Tunicate, *Doliolum nationalis*, phorozoid carrying two gonozooid buds (from shelf transect). (C) Cyclopoid copepod, *Oithona* sp. (note setose antennules and characteristic head-down orientation). (D) Calanoid copepod, *Centropages* sp. (adult male with geniculate right antennule). (E) Calanoid copepod, *Calanus* sp. (overwintering fifth-stage copepodite with oil storage sac). (F) Larvacean in mucous house. In (A) and (B), field of view = 7.0 mm; in (C) through (F), images from Gulf of Maine (41°15'N, 69°00'W) on 5 December 1991; field of view = 5.0 mm.

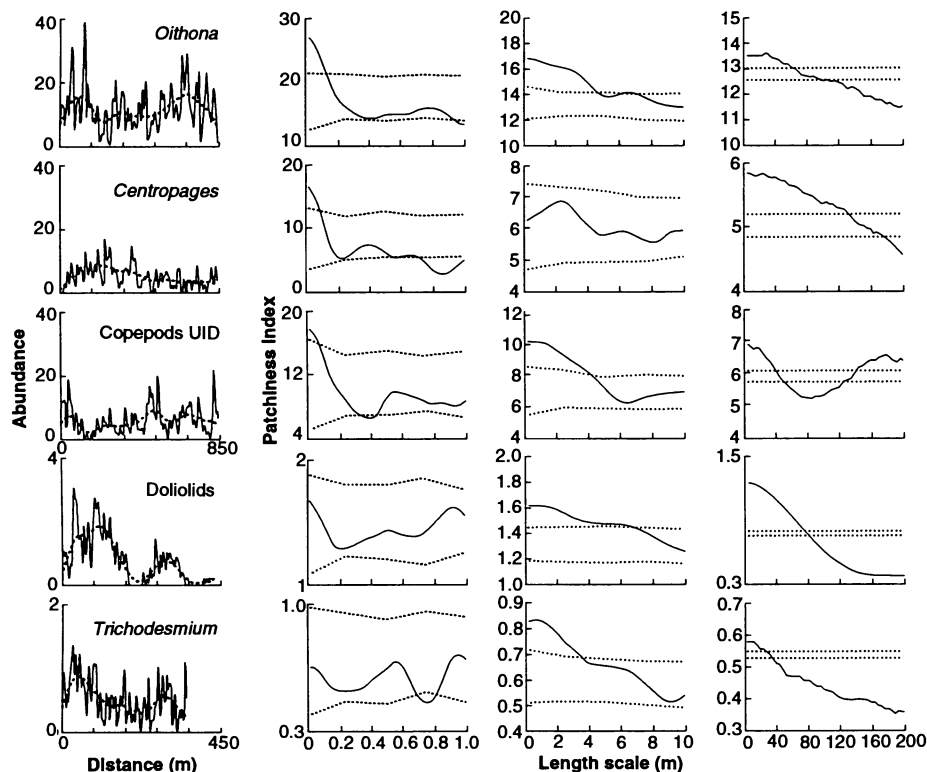
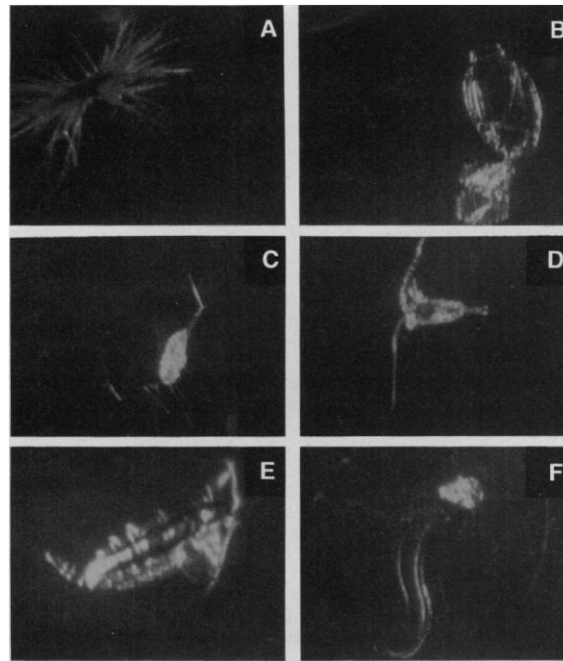


**Fig. 2.** Abundance and patchiness of dominant ring and shelf taxa. In abundance plots (first column), solid curve is data-smoothed with a 10-m window to remove microscale patchiness, whereas dotted curve is data-smoothed with a 100-m window. Abundance = number of plankton per liter of water. UID = unidentified. The three sets of panels on the right show the patchiness index (solid line) as a function of length scale for 1-, 10-, and 200-m domains; deviations of this index outside the 95% confidence intervals (dotted lines) indicate significant patchiness at that scale. Patchiness index = the mean number of plankton per liter of water. Deviations below the lower confidence interval indicate lower abundance than expected.

trophages at the larger scales, which suggests a common source of variability (probably physical).

Video data acquisition for plankton makes possible immediate, in situ observation of dominant taxa; such visual observations allow instant qualitative assessment of taxonomic composition in plankton communities. Given recent advances in video image processing including real-time digitization, thresholding, convolutions, and edge detection (12), real-time sorting of plankton into taxonomic categories will be possible in the near future. This will allow rapid quantitative mapping of plankton abundance together with taxonomic and size composition. Rapid acquisition of size-dependent taxonomic data over a range of scales in a dynamical oceanographic environment will provide new insights into the biological and physical processes controlling plankton populations in the sea.

## REFERENCES AND NOTES

1. B. J. Rothschild and C. G. H. Rooth, *Cooperative Institute for Marine and Atmospheric Studies Technical Report No. 82008* (University of Miami, Miami, FL, 1982).
2. Marine Zooplankton Colloquium, *Mar. Ecol. Prog. Ser.* **55**, 197 (1989).
3. W. J. Vlymen, *Environ. Biol. Fishes* **2**, 211 (1977).
4. C. S. Davis, G. R. Flierl, P. H. Wiebe, P. J. S. Franks, *J. Mar. Res.* **49**, 109 (1991).
5. M. R. Reeve, *J. Plankton Res.* **2**, 381 (1980).
6. Field data on spatial relationships among individual planktonic organisms are rare. Some statistical evidence for the existence of plankton micro-patchiness has been obtained with a towed bottle sampler [R. W. Owen, *J. Mar. Res.* **47**, 197 (1989)], but limited bottle number (15) and potential avoidance problems prevented estimates of patch size structure and interneighbor distances. Direct observations of certain larger pelagic organisms (>1 cm) such as medusae and krill have been made with the use of scuba and submersibles [C. E. Mills and J. Goy, *Bull. Mar. Sci.* **43**, 739 (1988); W. M. Hamner, P. P. Hamner, B. S. Obst, *Limnol. Oceanogr.* **34**, 451 (1989)], but direct observation and quantification of smaller organisms (<1 cm; that is, the bulk of the plankton) have proven difficult. Rough estimates of macrozooplankton (that is, ~3-mm *Calanus* sp.) abundance (number of organisms per square meter) have been obtained from a limited number of visual observations made with manned submersibles with a ruler mounted outside the viewing window. Avoidance problems and inability to see smaller plankton have made it difficult or impossible to use such systems for quantitative assessment of most plankton [A. L. Alldredge *et al.*, *Mar. Biol.* **80**, 75 (1984); G. O. Mackie and C. E. Mills, *Can. J. Fish. Aquat. Sci.* **40**, 763 (1983)]. High-magnification cinematographic observations of copepods have been made in the laboratory [J. R. Strickler, *Science* **218**, 158 (1982)]. More recently, vertical distributions of doliolids in the field were quantified with a low-magnification video camera (20-cm field) mounted on a submersible [G.-A. Paffenhöfer, *J. Plankton Res.* **13**, 971 (1991)]. Observation of plankton in situ at high magnification (<5 mm) has been difficult as a result of the relatively rapid motions and resultant image smearing at these scales.
7. The VPR consists of four video cameras with magnifying optics that we set for concentric viewing fields of 0.68, 1.78, 5.38, and 9.25 cm. Corresponding volumes were 0.9, 19.8, 200.0, and 636.4 ml ( $\pm 5\%$ ). The VPR is towed such that the flow is orthogonal to the camera-strobe axis. Resolution in the high-magnification viewing field was measured to be 10  $\mu\text{m}$ . An 80-W xenon strobe (pulse duration = 1  $\mu\text{s}$ ) was synchronized to match the video sampling rate of 60 fields per second. A long-pass, sharp-cut filter (>590 nm) was used on the strobe light to minimize risk of detection by plankton. The red light beam was expanded to 10 cm, collimated, and aimed obliquely past the cameras to provide dark-field illumination. Strobe to camera distance was 1.0 m with the viewing area at 0.5 m. Video data were telemetered to the surface via fiber-optic cable and stored, together with time code overlay, by the use of broadcast-quality video tape recorders. The VPR design is fully described elsewhere [C. S. Davis, S. M. Gallager, M. S. Berman, L. R. Haury, J. R. Strickler, *Arch. Hydrobiol.*, in press]. To minimize potential avoidance problems (8), we did not incorporate the gauze recorder box into the VPR, so that the 1.0-m space between the cameras and the strobe was free of obstructions.
8. The VPR was designed to minimize disturbance of the sampled volume in order to reduce possible disruption of the imaged particles or detection and avoidance by the plankton. Frontal area is much smaller than that of a comparably sized (1 m<sup>2</sup>) plankton net, and the imaged volume is located along the forward (upstream) edge of the instrument. Red light was used because zooplankton are known to be phototactic but are least sensitive to long wavelengths of light [K. V. Singarajah, *J. Mar. Biol. Assoc. U.K.* **55**, 627 (1975); J. H. Blaxter, *J. Exp. Biol.* **41**, 155 (1975)]. The large amount of open space between cameras and strobe (1.0 m) minimizes flow disturbance near the viewing area as determined by dye and avoidance studies in a tow tank [C. S. Davis and L. Haury, unpublished data]. In situ observations made in lower magnification cameras revealed that the organisms' trajectories, body orientation, and shape remained constant during transit through these windows, which indicates lack of flow distortion or escape response.
9. E. J. Carpenter and K. Romans, *Science* **254**, 1356 (1991); D. G. Capone and E. J. Carpenter, *ibid.* **217**, 1140 (1982); E. J. Carpenter, *Mar. Biol. Lett.* **4**, 6 (1983).
10. D. Deibel, *J. Mar. Res.* **43**, 211 (1985); *J. Plankton Res.* **4**, 143 (1982); *ibid.*, p. 189.
11. Given the binary nature of the data, standard spectral techniques using Fourier series could not be used to quantify variability as a function of spatial scale. The point process method used involved estimating the mean density of organisms at a distance,  $h$ , away from an individual [D. R. Cox and P. A. W. Lewis, *The Statistical Analysis of Series of Events* (Chapman and Hall, London, 1978)]. This was repeated for a range of  $h$  values to obtain a patchiness index as a function of length scale,  $P(h)$ . Patchiness indices were calculated separately for length scales of 1, 10, and 200 m. Confidence intervals (95%) were determined by calculating the patchiness index for each of 100 simulated random distributions. We found confidence intervals for 1- and 10-m scales by first smoothing the data with 8- and 80-m band widths, respectively, and then determining the patchiness index from simulations that randomized the smoothed data over length scales of 1 and 10 m. In this way, the patchiness index at smaller scales was unaffected by patchiness at larger scales. This method was also used across taxa to estimate correlations in abundance.
12. M. S. Berman, C. Katsinis, H. P. Jefferies, R. Lambert, *Eos* **71**, 94 (1990).
13. Supported by NSF grant OCE-9012657. We thank J. Kinder, P. Alatalo, B. Flannery, L. Haury, M. Gould, W. Lange, T. Silva, J. Strickler, the *Oceanus* crew, and the Woods Hole Oceanographic Institution (WHOI) facilities and graphics personnel for their inputs. We especially thank A. Morton, Sea Scan, Inc., North Falmouth, MA, for manufacturing the VPR according to our design. WHOI contribution 7928.

4 March 1992; accepted 18 May 1992

## Megascopic Eukaryotic Algae from the 2.1-Billion-Year-Old Negaunee Iron-Formation, Michigan

Tsu-Ming Han and Bruce Runnegar\*

Hundreds of specimens of spirally coiled, megascopic, carbonaceous fossils resembling *Grypania spiralis* (Walcott), have been found in the 2.1-billion-year-old Negaunee Iron-Formation at the Empire Mine, near Marquette, Michigan. This occurrence of *Grypania* is 700 million to 1000 million years older than fossils from previously known sites in Montana, China, and India. As *Grypania* appears to have been a photosynthetic alga, this discovery places the origin of organelle-bearing eukaryotic cells prior to 2.1 billion years ago.

Megascopic fossils resembling *Grypania spiralis* (Walcott) from the late Proterozoic of Montana (1, 2), China (2, 3), and India (4) occur within the lower part of the Negaunee Iron-Formation (IF), northern Michigan (Figs. 1 and 2). The Negaunee IF (Marquette Range) and correlative Biwabik

IF (Mesabi Range) have given an isotopic date (Sm-Nd isochron) of  $2110 \pm 52$  million years (5) and are early Proterozoic in age. This new horizon predates previously known occurrences of *Grypania* by 700 to 1000 million years; the fossils are the oldest known remains of megascopic organisms.

*Grypania spiralis* was a corkscrew-shaped, spaghetti-like organism that grew to maximum size of about half a meter in length and 2 mm in diameter (Fig. 3E). It is normally preserved as unbranched, ribbon-like films or impressions on bedding planes, but a unique specimen from India illustrated by Beer (6) is uncompact, showing

T.-M. Han, Research Laboratory, Cliffs Mining Services Company—Michigan, 504 Spruce Street, Ishpeming, MI 49849.

B. Runnegar, Department of Earth and Space Sciences, Molecular Biology Institute, and Institute of Geophysics and Planetary Physics, University of California, Los Angeles, CA 90024.

\*To whom correspondence should be addressed.